Journal of Non-Crystalline Solids 429 (2015) 24–32

Contents lists available at ScienceDirect

Journal of Non-Crystalline Solids

journal homepage: www.elsevier.com/ locate/ jnoncrysol

Crystallization of glass-forming liquids: Maxima of nucleation, growth, and overall crystallization rates

Jürn W.P. Schmelzer [a,*], Alexander S. Abyzov [b], Vladimir M. Fokin [c,d], Christoph Schick [a], Edgar D. Zanotto [d]

[a] Institut für Physik der Universität Rostock, Wismarsche Strasse 43-45, 18057 Rostock, Germany
[b] National Science Center Kharkov Institute of Physics and Technology, 61108 Kharkov, Ukraine
[c] Vavilov State Optical Institute, ul. Babushkina 36-1, 193 171 St. Petersburg, Russia
[d] Vitreous Materials Laboratory, Department of Materials Engineering, Federal University of São Carlos, UFSCar, 13565-905, São Carlos, SP, Brazil

ARTICLE INFO

Article history:
Received 8 June 2015
Received in revised form 16 August 2015
Accepted 19 August 2015
Available online xxxx

Jel classification:
Liquids
Glasses
Crystals

PACS numbers:
64.60.Bd General theory of phase transitions;
64.60.Q– Nucleation;
81.10.Aj Theory and models of crystal growth;
64.70.kj Glasses

Keywords:
Nucleation;
Crystal growth;
Overall crystallization

ABSTRACT

A set of equations for determining the temperatures and magnitudes of the maximum nucleation, growth, and overall crystallization rates of glass-forming liquids is derived and analyzed. The analysis is performed based on the classical theories of nucleation and growth, without introducing additional assumptions such as the Stokes–Einstein–Eyring (SEE) equation, models for specific kinetic mechanisms of aggregation, a specification of the type of temperature dependence of the diffusion coefficient, or specific models for the computation of the driving force of crystallization and the work of critical cluster formation. Such approximations are employed only for analytical estimates and to illustrate the general results. In particular, it is shown that the magnitude of the maximum of the steady-state nucleation rate J_{max} decreases upon increasing the ratio $T_{max}^{(nucl)}/T_m$ ($T_{max}^{(nucl)}$: temperature of maximum of the steady-state nucleation rate, T_m: melting or liquidus temperature). Similarly, the maximum growth rate, u_{max}, decreases with increasing values of the ratio $T_{max}^{(growth)}/T_m$ ($T_{max}^{(growth)}$: temperature of maximum of the growth rate). Several experimental results on the crystallization kinetics of glass-forming liquids are interpreted theoretically for the first time employing the concepts developed here.

1. Introduction

The properties of materials are significantly affected by the volume fraction, shape, size distribution, orientation, and degree of dispersion of the different phases formed during their fabrication [1,2]. Crystallization is particularly important in glass technology, where, in addition to the aforementioned features, the rates of crystal nucleation and growth of glass-forming melts determine whether a given liquid can be vitrified or is likely to crystallize on the cooling path [3–5].

To control the features of the newly evolving phases in an undercooled liquid and the characteristics of the resulting material, an in-depth understanding of the mechanisms of nucleation and crystal growth is required [2,3,6]. A detailed knowledge about the location and magnitude of the maxima of the nucleation, growth, and overall crystallization rates as a function of temperature or other thermodynamic control parameters, such as pressure, is of particular importance in this respect [7]. For instance, knowledge of the temperatures of the nucleation and growth rate maxima is a prerequisite to use Tammann's development method, which is widely employed for the experimental determination of steady-state crystal nucleation rates [8–10]. The location and magnitude of the maximum nucleation and growth rates widely determine the crystallizability of a glass-forming melt in cooling. In the present paper, we consider the dependence of these maxima on temperature at a fixed pressure. This analysis can be easily extended to similar situations, such as variations of pressure at constant temperature.

Phase formation processes are till now mainly described employing the classical theories of nucleation and growth [2,3,6,11]. Based on the knowledge of the macroscopic bulk and surface properties (such as free energy density differences between liquid and crystal phases and specific interfacial energy) of the substances under consideration and the viscosity of the undercooled liquid, this theory provides a qualitative (and partly quantitative) explanation of crystallization phenomena. The

* Corresponding author.
E-mail address: juern-w.schmelzer@uni-rostock.de (J.W.P. Schmelzer).

http://dx.doi.org/10.1016/j.jnoncrysol.2015.08.023
0022-3093/

classical theory is also employed here, however, the general relations that determine the location and magnitude of the maxima of rates of nucleation, growth, and overall crystallization are derived independently of any assumptions concerning the properties of the evolving crystallites. In addition, in deriving the general relations and analyzing them, we do not use any specific equations for the temperature dependence of the diffusion coefficient or the viscosity, such as the Vogel–Fulcher–Tammann (VFT) equation, for example. In addition, we do not assume validity of the Stokes–Einstein–Eyring (SEE) equation in the derivation of the basic relations. This relation is frequently employed in the description of crystal nucleation and growth, allowing one to replace the effective diffusion coefficients, D governing nucleation and growth, by the Newtonian viscosity, $\eta(T)$. However, it is applicable only for sufficiently high temperatures above a specific for a given system decoupling temperature, T_d (cf. [2,3,9]). While the existence of the maxima of nucleation and growth rates is qualitatively known to result from the interplay between the decrease of the effective diffusion coefficient (increase of the viscosity when the SEE-equation holds) and the decrease of the work of critical cluster formation (due to the increase of the thermodynamic driving force of crystallization with decreasing temperature) with decreasing temperature, to the best of our knowledge, a quantitative theoretical analysis is performed here in general terms for the first time. Only after having performed the analysis in the aforementioned general manner, we illustrate the general relations derived here by employing specific assumptions concerning the thermodynamic and kinetic parameters of the system under consideration.

For illustration purposes, a simple thermodynamic model is utilized here for the description of the crystallites. This model can be extended in different directions in order to arrive at a more accurate interpretation of experimental data [2,3,12–18]. The choice of description of the thermodynamic factors that determine nucleation and growth employed here affects the results quantitatively, but not qualitatively, since the general results are obtained independently of these assumptions. Consequently, the general trends established here theoretically in terms of the classical theory of nucleation and growth, and illustrated based on a relatively simple model, may also serve as a guide in more complex situations as will be demonstrated in subsequent contributions.

The paper is structured as follows: In Section 2 the basic equations for the description of crystal nucleation and growth are formulated. These relations are used in Section 3 to determine the temperatures and magnitude of the maxima of nucleation, growth, and overall crystallization rates. The results are applied to the interpretation of a wide spectrum of experimental data. A discussion of the results and possible developments, given in Section 4, completes the paper.

2. Basic equations

2.1. General relations

As outlined in the introduction, our analysis is performed in terms of the classical theories of nucleation and growth utilizing, for illustration purposes, commonly employed approximations to describe the properties of the systems under consideration [3,12]. The steady-state nucleation rate, J, is expressed as

$$J = c\sqrt{\frac{\sigma}{k_B T}}\left(\frac{D}{d_0}\right)\exp\left(-\frac{W_c}{k_B T}\right) \quad . \tag{1}$$

Here, σ is the specific interfacial energy, k_B the Boltzmann constant, T the absolute temperature, D the effective diffusion coefficient governing the processes of aggregation of ambient phase particles to crystal clusters, and d_0 is a characteristic size parameter that is determined by the particle number density, c, of the basic units of the ambient phase ($c = (1/d_0^3)$). It is assumed that the particle number densities are the same in both phases, i.e., density differences and elastic stresses resulting from them are neglected.

In the case of homogeneous nucleation of spherical nuclei, the size of the critical cluster, R_c, its surface area, A_c, and the work of critical cluster formation, W_c, are given by the following relations

$$R_c \cong \frac{2\sigma}{c\Delta\mu}, \qquad W_c = \frac{1}{3}\sigma A_c = \frac{16\pi}{3}\frac{\sigma^3}{(c\Delta\mu)^2}, \qquad A_c = 4\pi R_c^2. \tag{2}$$

Here, $\Delta\mu$ is the difference in the chemical potential per particle in the liquid and the crystal.

Solid particles may trigger heterogeneous nucleation. With respect to the work of critical cluster formation, the effect of such nucleation cores can be accounted for by the introduction of the nucleation activity factor, Φ, to the work of homogeneous critical cluster formation. This factor is always smaller than unity [3]:

$$W_c^{het} = W_c\Phi \ , \qquad \Phi < 1. \tag{3}$$

In addition, to compute the steady-state heterogeneous nucleation rate, the particle number density, c (which represents the number of homogeneous nucleation sites), must be replaced in the expression for J, Eq. (1), by the number of solid nucleation cores, c_{het}, that may act as centers of heterogeneous nucleation.

For the macroscopic linear growth rate, u, we use the commonly employed relation [19,20]

$$u = f\frac{D}{4d_0}\left[1-\exp\left(-\frac{\Delta\mu}{k_B T}\right)\right] \ , \tag{4}$$

where $f \le 1$ is a parameter that has different values for different modes of growth. We suppose that the kinetics of aggregation is the same for both nucleation and growth and is governed by a diffusion coefficient, D, which can be written as

$$D = D_0\exp\left(-\frac{E_D}{k_B T}\right) \ . \tag{5}$$

The activation energy for diffusion, $E_D = E_D(T)$, depends on temperature, pressure, and composition. Pressure and composition are assumed to be constant and not affected by the phase formation processes considered.

2.2. Approximations

We derive the basic relations for the determination of the maxima of nucleation, growth, and overall crystallization rates based on the general relations summarized in Section 2.1. For illustration and analytical estimates, we employ a simple model, which can be easily generalized if necessary (cf. [2,3]). Here, we express the thermodynamic driving force, $\Delta\mu$, for nucleation and growth in its simplest form as

$$\Delta\mu = q\left(1-\frac{T}{T_m}\right), \qquad q = T_m\Delta s_m \ , \tag{6}$$

where q ($q > 0$) is the latent heat of crystallization per particle and Δs_m is the melting entropy per particle at the equilibrium melting (or liquidus) temperature, T_m. This expression gives an upper bound for $\Delta\mu$, the experimentally determined values of $\Delta\mu$ are always smaller than the ones calculated by Eq. (6) (cf. also Eqs. (6.62)–(6.65) in [3]).

The specific surface energy, σ, is estimated by the Stefan–Skapski–Turnbull relation [3] as

$$\sigma = \alpha\frac{q}{v^{2/3}}, \qquad v = \frac{1}{c} = d_0^3. \tag{7}$$

Employing this relation, surface effects enter the description via the parameter α. For different systems, this parameter was

found to have values commonly in the range $0.3 < \alpha < 0.6$ [3]. For a given system, the specific surface energy and the parameter α may also depend on temperature [6,21]; however, in illustrating the general results here these two parameters are considered to be constant.

With above described relations and assumptions, the work of critical cluster formation can be expressed as

$$\frac{W_c}{k_B T_m} = \frac{\Omega}{\left(1-\frac{T}{T_m}\right)^2}, \qquad \Omega = \frac{16\pi\alpha^3\Phi}{3}\left(\frac{q}{k_B T_m}\right). \tag{8}$$

This relation accounts for both homogeneous ($\Phi = 1$) and heterogeneous ($\Phi < 1$) nucleation. Employing these notations, the steady-state nucleation rate is given by

$$J \cong c\sqrt{\left(\frac{\alpha q}{k_B T_m}\right)}\left(\frac{D}{d_0^2}\right)\exp\left(-\frac{\Omega}{\frac{T}{T_m}\left(1-\frac{T}{T_m}\right)^2}\right). \tag{9}$$

In this equation, only one parameter reflects the bulk properties of the substance under consideration, the ratio of the latent heat, $q(T_m)$, divided by the characteristic thermal energy, $k_B T_m$.

3. Determination of the maxima of nucleation, growth, and overall crystallization rates

3.1. Temperature at maximum nucleation rate

3.1.1. Derivation

Combining Eqs. (1) and (5), we may express the steady-state nucleation rate as

$$J = c\sqrt{\frac{\sigma}{k_B T}}\left(\frac{D_0}{d_0}\right)\exp\left(-\frac{W_c + E_D}{k_B T}\right). \tag{10}$$

In determining the temperature and magnitude of the maximum nucleation rate, we – following Frenkel [22] and Filipovich [23] – consider the pre-exponential term in Eq. (10) to be only weakly temperature-dependent in comparison with the exponential term. In such an approach, the temperature $T_{max}^{(nucl)}$ at the maximum nucleation rate corresponds to the minimum of the ratio $(W_c + E_D)/k_B T$ and is defined by

$$\frac{d}{dT}\left(\frac{W_c + E_D}{T}\right)\Big|_{T=T_{max}^{(nucl)}} = \frac{1}{T^2}\left\{T\frac{d(W_c + E_D)}{dT} - (W_c + E_D)\right\}\Big|_{T=T_{max}^{(nucl)}} = 0. \tag{11}$$

We thus arrive at the general result

$$\frac{T_{max}^{(nucl)}}{T_m} = \frac{1}{T_m}\left(\frac{W_c + E_D}{\frac{d(W_c+E_D)}{dT}}\right)\Big|_{T=T_{max}^{(nucl)}}. \tag{12}$$

Employing the approximations that lead to Eq. (8), this relation can be transformed to

$$\frac{T_{max}^{(nucl)}}{T_m} = \left(\frac{W_c + \left(E_D - T\frac{dE_D}{dT}\right)}{3W_c + \left(E_D - T\frac{dE_D}{dT}\right)}\right)\Big|_{T=T_{max}^{(nucl)}}. \tag{13}$$

As a rule, one can expect (cf. Eq. (2.80) in [3]) that the inequality

$$\frac{dE_D(T)}{dT} \le 0 \tag{14}$$

holds. An account of the temperature dependence of the activation energy leads, consequently, to higher values of the effective activation energy for diffusion, $E_D^{(eff)}(T)$, defined by

$$E_D^{(eff)}(T) = \left(E_D(T) - T\frac{dE_D(T)}{dT}\right), \tag{15}$$

as compared with E_D, i.e., the inequality

$$E_D^{(eff)}(T) \ge E_D(T) \tag{16}$$

holds (cf. [24]). Employing the notation of an (with respect to the specification of $T_{max}^{(nucl)}$) effective activation energy of diffusion, defined by Eq. (15), Eq. (13) yields

$$\frac{T_{max}^{(nucl)}}{T_m} = \left(\frac{W_c(T) + E_D^{(eff)}(T)}{3W_c(T) + E_D^{(eff)}(T)}\right)\Big|_{T=T_{max}^{(nucl)}}. \tag{17}$$

In the limiting case of constant activation energy for diffusion, $(dE_D/dT) \cong 0$, we arrive at the approximate relationship

$$\frac{T_{max}^{(nucl)}}{T_m} \cong \left(\frac{W_c(T) + E_D}{3W_c(T) + E_D}\right)\Big|_{T=T_{max}^{(nucl)}} \quad \text{at} \quad \frac{dE_D}{dT} \cong 0, \tag{18}$$

which was earlier derived by Filipovich [23] (cf. also [3]).

The following general conclusions can be drawn from Eqs. (12), (17), and (18): (i) For any value of $T_{max}^{(nucl)}$ and $W_c(T_{max}^{(nucl)})$, an increase of E_D and, thus, of $E_D^{(eff)}$, leads to higher values of $T_{max}^{(nucl)}/T_m$. For the same value of E_D, (ii) systems characterized by a temperature-dependent activation energy have the maximum of the steady-state nucleation rates at higher $T_{max}^{(nucl)}/T_m$ and, as will be demonstrated in the subsequent section, (iii) lower values of $J_{max}(T_{max}^{(nucl)})$.

According to the considerations outlined above, the necessary conditions for a maximum of the steady-state nucleation rate are given by Eq. (11). The respective sufficient condition for the existence of a maximum of the nucleation rate (minimum of $(W_c + E_D)/T$) results in

$$\frac{d^2}{dT^2}\left(\frac{W_c + E_D}{T}\right)\Big|_{T=T_{max}^{(nucl)}} > 0. \tag{19}$$

As a direct consequence, this relation yields

$$\frac{d^2}{dT^2}(W_c + E_D)\Big|_{T=T_{max}^{(nucl)}} > 0. \tag{20}$$

3.1.2. Correlation between J_{max} and $T_{max}^{(nucl)}/T_m$

To study the dependence of the maximum value of the steady-state nucleation rate, J_{max}, on $T_{max}^{(nucl)}$, in the general case we may utilize Eqs. (10) and (12). By combining them, we obtain

$$J_{max}\left(T_{max}^{(nucl)}\right) \propto \exp\left(-\frac{W_c + E_D}{k_B T}\right)\Big|_{T=T_{max}^{(nucl)}} \propto \exp\left(-\frac{d(W_c + E_D)}{k_B dT}\right)\Big|_{T=T_{max}^{(nucl)}} \tag{21}$$

resulting, with the inequality Eq. (20) (which is a consequence of Eq. (19)), in

$$\frac{d}{dT_{max}^{(nucl)}}\left(J_{max}\left(T_{max}^{(nucl)}\right)\right) \propto \left(-\frac{d^2(W_c + E_D)}{dT^2}\right)\Big|_{T=T_{max}^{(nucl)}} < 0. \tag{22}$$

It follows that the magnitude of the maximum steady-state nucleation rate generally decreases when the ratio $(T_{max}^{(nucl)}/T_m)$ increases.

To illustrate this generally valid result, we first reformulate Eq. (10) as

$$J_{max}\left(T_{max}^{(nucl)}\right) = c\sqrt{\frac{\sigma}{k_B T}}\left(\frac{D_0}{d_0}\right)\exp\left\{-\left(\frac{E_D(T)}{k_B T_m}\right)\frac{\left(\frac{W_c(T)}{E_D(T)}\right)+1}{\left(\frac{T}{T_m}\right)}\right\}\Bigg|_{T=T_{max}^{(nucl)}}. \quad (23)$$

In the limiting case that the driving force for crystallization is given by Eq. (6) and the activation energy for diffusion is independent of temperature, we can employ Eq. (18) to replace $(T_{max}^{(nucl)}/T_m)$ by (W_c/E_D). We thus obtain

$$J_{max}\left(T_{max}^{(nucl)}\right) = c\sqrt{\frac{\sigma}{k_B T_{max}^{(nucl)}}}\left(\frac{D_0}{d_0}\right)\exp\left\{-\frac{E_D}{k_B T_m}\left(3\frac{W_c\left(T_{max}^{(nucl)}\right)}{E_D}+1\right)\right\}. \quad (24)$$

Because the work of critical cluster formation is a monotonically increasing function of temperature (cf. Eq. (8)), the value of the steady-state nucleation rate at the maximum of the $J(T)$-curve decreases with increasing $T_{max}^{(nucl)}$. This type of behavior is illustrated in Fig. 1.

The curves in Fig. 1 are obtained as follows. First, we rewrite Eq. (24) in the form of

$$J_{max}\left(\frac{T_{max}^{(nucl)}}{T_m}\right) = J_0\exp\left(-\frac{E_D}{k_B T_m}\right)\exp\left(-3\frac{W_c\left(T_{max}^{(nucl)}\right)}{k_B T_m}\right), \qquad J_0 = c\sqrt{\frac{\sigma}{k_B T_{max}^{(nucl)}}}\left(\frac{D_0}{d_0}\right). \quad (25)$$

We consider the pre-factor J_0 in Eq. (25) as constant, again, compared with the exponential terms. We then fix a certain value of the ratio $(T_{max}^{(nucl)}/T_m)$ and via Eq. (8) determine the work of critical cluster formation, W_c, corresponding to this temperature. Accordingly, we must assign appropriate values to the parameter Ω (cf. Eq. (8)) that reflects specific properties of the system under consideration. Employing Eqs. (8) and (18), we can also determine the particular value of the activation energy for diffusion, E_D, corresponding to the selected value of $(T_{max}^{(nucl)}/T_m)$. We arrive at

$$\frac{E_D}{k_B T_m} = \Omega\frac{3\left(\frac{T_{max}^{(nucl)}}{T_m}\right)-1}{1-\left(\frac{T_{max}^{(nucl)}}{T_m}\right)^3}. \quad (26)$$

By such procedure, the dependence of $J_{max}(T_{max}^{(nucl)}/T_m)$ on $(T_{max}^{(nucl)}/T_m)$ can be established for all values of $(T_{max}^{(nucl)}/T_m)$, where such a maximum exists.

The necessary condition for the existence of a maximum for a given value of $(T_{max}^{(nucl)}/T_m)$ consists of the existence of a positive value of E_D in Eq. (26). According to this equation, Eq. (26) (consistent with Eq. (18)), the maximum steady-state nucleation rate may be located in the temperature range of (cf. [20,23])

$$\frac{1}{3} < \left(\frac{T_{max}^{(nucl)}}{T_m}\right) < 1. \quad (27)$$

The value of the parameter E_D which corresponds to the selected value of $(T_{max}^{(nucl)}/T_m)$ is, according to Eq. (26), a monotonically increasing function of the ratio $(T_{max}^{(nucl)}/T_m)$. It is equal to zero in the limit $(T_{max}^{(nucl)}/T_m) = 1/3$ and approaches infinity in the limit $(T_{max}^{(nucl)}/T_m) \to 1$. It follows that – within the range of temperatures specified by Eq. (27) – higher values of E_D yield larger values of $(T_{max}^{(nucl)}/T_m)$.

The latter result also holds true when E_D depends on temperature. Indeed, in this more general case, we arrive at

$$J_{max} = c\sqrt{\frac{\sigma}{k_B T_{max}^{(nucl)}}}\left(\frac{D_0}{d_0}\right)\exp\left\{-\frac{1}{k_B T_m}\left(\frac{W_c+E_D}{W_c+E_D^{(eff)}}\right)\left(3W_c\left(T_{max}^{(nucl)}\right)+E_D^{(eff)}\right)\right\}, \quad (28)$$

or, to a good approximation, at

$$J_{max} \cong c\sqrt{\frac{\sigma}{k_B T_{max}^{(nucl)}}}\left(\frac{D_0}{d_0}\right)\left\{\exp\left(-\frac{E_D^{(eff)}\left(T_{max}^{(nucl)}\right)}{k_B T_m}\right)\exp\left(-3\frac{W_c\left(T_{max}^{(nucl)}\right)}{k_B T_m}\right)\right\}. \quad (29)$$

Now, it is not the parameter E_D but $E_D^{(eff)}$ that must be determined. This calculation can be performed in the same way as when E_D is independent of temperature. Consequently, the results for the dependence of J_{max} on $T_{max}^{(nucl)}$ must again have the same form as those shown in Fig. 1.

From the above derived dependencies it follows that low values of the effective activation energy, $E_D^{(eff)}$, at T_m and low values of its rate of change with temperature result in higher values of J_{max} because the maximum is reached at lower values of $T_{max}^{(nucl)}$ and correspondingly at higher undercooling (lower values of the work of critical cluster formation). Taking into account the temperature dependence of the activation energy, the maximum of the steady-state nucleation rate is shifted to higher temperatures. Consequently, the nucleation rate at the maximum is smaller than in the case of constant activation energies for diffusion. This result can also be formulated in a different way: High activation energies for diffusion at T_m result in higher values of $T_{max}^{(nucl)}$ and, correspondingly, in lower values of J_{max}.

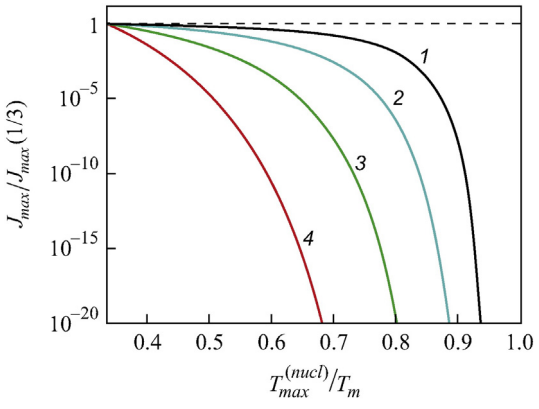

Fig. 1. Dependence of the maximum steady-state nucleation rate, $J_{max}(T_{max}^{(nucl)}/T_m)$, on the reduced temperature, $(T_{max}^{(nucl)}/T_m)$, for different values of the parameter Ω reflecting the properties of the system under consideration. The steady-state nucleation rate is given in a reduced form $J_{max}(T_{max}^{(nucl)}/T_m)/J_{max}^{(nucl)}((T_{max}^{(nucl)}/T_m) = 1/3)$. To the parameter $\Omega = (16\pi\alpha^3\Phi/3)(q/k_B T_m)$ (cf. Eq. (8)), the following values have been assigned: (1) Ω = 0.064, (2) Ω = 0.212, (3) Ω = 0.636, (4) Ω = 1.908.

3.2. Temperature at maximum growth rate

3.2.1. Derivation

The temperature at the maximum growth rate, $T_{max}^{(growth)}$, is determined by setting in Eq. (4) $(du/dT) = 0$. We obtain

$$\left\{\frac{d\ln D}{dT}\left[1-\exp\left(-\frac{\Delta\mu}{k_BT}\right)\right]+\exp\left(-\frac{\Delta\mu}{k_BT}\right)\frac{d}{dT}\left(\frac{\Delta\mu}{k_BT}\right)\right\}\Bigg|_{T=T_{max}^{(growth)}}=0\ , \tag{30}$$

$$\frac{d}{dT}\left(\frac{E_D}{T}\right)\left(\exp\left(\frac{\Delta\mu}{k_BT}\right)-1\right)\Bigg|_{T=T_{max}^{(growth)}}=\frac{d}{dT}\left(\frac{\Delta\mu}{T}\right)\Bigg|_{T=T_{max}^{(growth)}}, \tag{31}$$

or, equivalently,

$$E_D^{(eff)}\left(T_{max}^{(growth)}\right)=-\frac{\Delta\mu}{\exp\left(\frac{\Delta\mu}{k_BT}\right)-1}\left(\frac{T}{\Delta\mu}\frac{d\Delta\mu}{dT}-1\right)\Bigg|_{T=T_{max}^{(growth)}}. \tag{32}$$

In the derivations, it is again assumed that D_0 is not dependent on temperature.

Employing Eq. (6), the generally valid result, given by Eq. (32), can be simplified to

$$\exp\left(\frac{\Delta\mu}{k_BT}\right)\Bigg|_{T=T_{max}^{(growth)}}=1+\frac{q}{E_D^{(eff)}}\Bigg|_{T=T_{max}^{(growth)}}. \tag{33}$$

Resolving this relation with respect to $(T_{max}^{(growth)}/T_m)$, we obtain

$$\frac{T_{max}^{(growth)}}{T_m}=\frac{1}{1+\frac{k_BT_m}{q}\ln\left(1+\frac{q}{E_D^{(eff)}}\right)}\Bigg|_{T=T_{max}^{(growth)}}. \tag{34}$$

This equation can be approximated to

$$\frac{T_{max}^{(growth)}}{T_m}\cong\frac{1}{1+\left(\frac{k_BT_m}{E_D^{(eff)}}\right)}\Bigg|_{T=T_{max}^{(growth)}}\cong 1-\left(\frac{k_BT_m}{E_D^{(eff)}}\right)\Bigg|_{T=T_{max}^{(growth)}}. \tag{35}$$

In addition, assuming that E_D is independent of temperature, we arrive at

$$\frac{T_{max}^{(growth)}}{T_m}\cong\frac{1}{1+\left(\frac{k_BT_m}{E_D}\right)}\cong 1-\left(\frac{k_BT_m}{E_D}\right)\ . \tag{36}$$

According to Eqs. (4) and (30), the sign of the second-order derivative of the growth rate at the extremum is given by

$$\left.\frac{d^2u}{dT^2}\right|_{T=T_{max}^{(growth)}}=\left(\frac{fD}{4d_0}\right)\frac{d}{dT}\left\{\frac{d\ln D}{dT}\left[1-\exp\left(-\frac{\Delta\mu}{k_BT}\right)\right]+\right.$$
$$\left.+\exp\left(-\frac{\Delta\mu}{k_BT}\right)\frac{d}{dT}\left(\frac{\Delta\mu}{k_BT}\right)\right\}\Bigg|_{T=T_{max}^{(growth)}}, \tag{37}$$

resulting in

$$\left.\frac{d^2u}{dT^2}\right|_{T=T_{max}^{(growth)}}=\left(\frac{fD}{4d_0}\right)\left\{\frac{d^2\ln D}{dT^2}\left[1-\exp\left(-\frac{\Delta\mu}{k_BT}\right)\right]-\right.$$
$$\left.-\frac{q}{k_BT^2}\exp\left(-\frac{\Delta\mu}{k_BT}\right)\frac{d\ln D}{dT}-\frac{q}{k_B}\frac{d}{dT}\left[\frac{1}{T^2}\exp\left(-\frac{\Delta\mu}{k_BT}\right)\right]\right\}\Bigg|_{T=T_{max}^{(growth)}}, \tag{38}$$

or, employing Eq. (33), in

$$\left.\frac{d^2u}{dT^2}\right|_{T=T_{max}^{(growth)}}=-\left(\frac{fD}{4d_0}\right)\exp\left(-\frac{\Delta\mu}{k_BT}\right)\left(\frac{q}{k_BT^3}\right)\left\{q+E_D^{(eff)}-\frac{d\ln E_D^{(eff)}}{d\ln T}\right\}\Bigg|_{T=T_{max}^{(growth)}}. \tag{39}$$

With Eq. (14), this result confirms that Eqs. (32)–(36) determine the temperature at the maximum growth rate.

3.2.2. Correlation between u_{max} and $T_{max}^{(growth)}/T_m$

Based on a comprehensive analysis of available experimental data, Orava and Greer [25] have recently shown that "*for all glass-forming systems, the maximum value of the crystal growth rate u_{max} is correlated with the homologous temperature $(T_{max}^{(growth)}/T_m)$ at which the maximum occurs*" (cf. Fig. 2 in [25]). We will now show that this result can be explained straightforwardly in terms of the above derived relations.

According to Eq. (4), the maximum growth rate, u_{max}, can be written as

$$u_{max}\left(T_{max}^{(growth)}\right)=f\frac{D\left(T_{max}^{(growth)}\right)}{4d_0}\left[1-\exp\left(-\frac{\Delta\mu\left(T_{max}^{(growth)}\right)}{k_BT_{max}^{(growth)}}\right)\right]. \tag{40}$$

With the general relation, Eq. (33), we obtain

$$1-\exp\left(-\frac{\Delta\mu}{k_BT}\right)\Bigg|_{T=T_{max}^{(growth)}}=\frac{\frac{q}{E_D^{(eff)}}}{1+\frac{q}{E_D^{(eff)}}}\Bigg|_{T=T_{max}^{(growth)}}. \tag{41}$$

A substitution into Eq. (40) accounting for Eq. (4) yields

$$u_{max}\left(T_{max}^{(growth)}\right)=f\frac{D_0}{4d_0}\left(\frac{\frac{q}{E_D^{(eff)}}}{1+\frac{q}{E_D^{(eff)}}}\right)\exp\left[\left(-\frac{E_D}{k_BT_m}\right)\left(\frac{T_m}{T_{max}^{(growth)}}\right)\right]\Bigg|_{T=T_{max}^{(growth)}}. \tag{42}$$

Employing the first of the approximations given in Eq. (36), we can replace the ratio (E_D/k_BT_m) in the exponential term in Eq. (42), resulting in

$$u_{max}\left(T_{max}^{(growth)}\right)\cong f\frac{D_0}{4d_0}\left(\frac{\frac{q}{E_D^{(eff)}}}{1+\frac{q}{E_D^{(eff)}}}\right)\exp\left(-\frac{1}{1-\left(\frac{T_{max}^{(growth)}}{T_m}\right)}\right)\Bigg|_{T=T_{max}^{(growth)}}. \tag{43}$$

Fig. 2 illustrates the dependence of the maximum value of the crystal growth rate u_{max} on the reduced temperature $T_{max}^{(growth)}/T_m$ obtained based on Eq. (43). The calculations were performed for two different growth mechanisms. The red line corresponds to *normal growth*, and the blue line refers to *screw-dislocation mediated growth*. The symbols refer to data for different systems given in [25] supplemented with data from other sources. For oxide glasses revealing stoichiometric crystallization (glass and crystals have the same composition) the temperatures of maximum growth rates were also calculated by Eq. (43) using the experimentally determined values of u_{max} and plotted together with experimentally measured $T_{max}^{(growth)}$-values. Taking into account the relatively flat shape of the maximum of crystal growth rates in the range of $T_{max}^{(growth)}$ and also the possible underestimation of the crystal/melt interface temperature, the agreement between $T_{max}^{(growth)}$ measured experimentally and determined theoretically is quite reasonable.

Our computations are equivalent to the curve drawn by Orava and Greer (full curve in Fig. 2 in [25]) given there as a guide for the eye, only. Consequently, their master curve can be given a theoretical foundation as a direct result (mainly) of the exponential term in Eq. (43), which depends exclusively on the ratio $T_{max}^{(growth)}/T_m$. Deviations of the experimental data from their master curve and from our computations

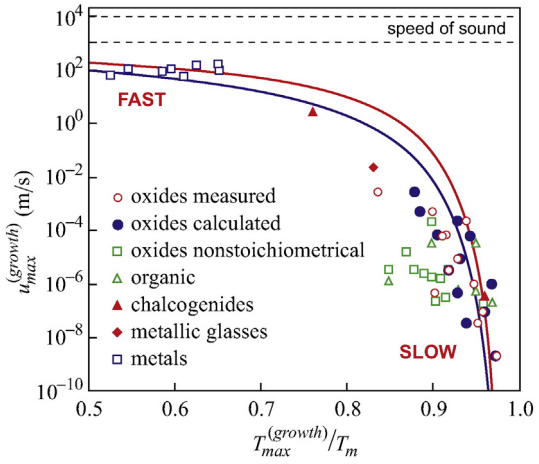

Fig. 2. Dependence of the maximum crystal growth rate, u_{max}, on the reduced temperature, $T_{max}^{(growth)}/T_m$, at which the maximum computed via Eq. (43) occurs. The red line refers to normal growth, while the blue line describes screw dislocation mediated growth. The following typical values of the parameters are employed for the computations: $D_0 = 4 \cdot 10^{-6}$ m^2/s, $d_0 = 3.895 \cdot 10^{-10}$m, $q = 1.235 \cdot 10^{-19}$J, and $E_D = 1.6 \cdot 10^{-19}$J. The symbols refer to different systems given in [25] and are slightly modified here. We added experimental growth rate data only for stoichiometric silicate systems. Experimental errors for $T_{max}^{(growth)}/T_m$ and u_{max} in these systems are not higher that 1% and 10–20%, respectively. In scale of Fig. 2 these errors are comparable with the data point's size. The aim of this figure is mainly to illustrate the general trend and how it can be explained by the equations derived by us. Following [25], the speed of sound is indicated which sets a physical limit to the crystal-growth rate.

(cf. Fig. 2) can be assigned to a temperature dependence of the activation energy and to specific features of the different systems described by the first factors in Eqs. (43) and (44). In particular, our computations can be further extended by utilizing the more correct (as compared to Eq. (36)) relations, Eqs. (34) and (35), or by improving the model used to describe the properties of the crystals. For example, employing the more correct relation, Eq. (35), instead of Eq. (36), we arrive at

$$u_{max} \cong f \frac{D_0}{4d_0} \left(\frac{\frac{q}{E_D^{(eff)}}}{1 + \frac{q}{E_D^{(eff)}}} \right) \exp\left\{ -\left(\frac{1}{1 - \left(\frac{T_{max}^{(growth)}}{T_m} \right)} + \frac{d}{dT}\left(\frac{E_D}{k_B} \right) \right) \right\} \Bigg|_{T=T_{max}^{(growth)}} . \quad (44)$$

The additional term in Eq. (44) compared with Eq. (43) shifts the growth rate curve to higher magnitudes (cf. Eq. (14)). The growth kinetics may also be affected by the release of latent heat of crystallization and the resulting temperature fields at the crystal–liquid interface.

Here, we will not attempt to further develop such a quantitatively more correct description (which necessarily involves additional assumptions) because the basic result is already described by the simplest relation, Eq. (43). Note also that the determination of the location of the temperature corresponding to the maximum growth rate is confronted with certain experimental problems because the maximum is normally spread over a relatively wide temperature range.

3.3. Relative locations of the temperatures at maximum nucleation and growth rates

The difference $(T_{max}^{(growth)} - T_{max}^{(nucl)})$ between the temperature at the maximum rates of crystal growth and nucleation can be computed for any given system via Eqs. (12) and (32). To derive analytical relations allowing one to arrive directly at conclusions concerning the sign of this temperature difference, we also present here a simplified approach involving reasonable approximations. In particular, from Eqs. (17) and (35) we obtain

$$\frac{T_{max}^{(growth)} - T_{max}^{(nucl)}}{T_m} \cong 1 - \left(\frac{k_B T_m}{E_D^{(eff)}} \right) \Bigg|_{T=T_{max}^{(growth)}} - \left(\frac{W_c + E_D^{(eff)}}{3W_c + E_D^{(eff)}} \right) \Bigg|_{T=T_{max}^{(nucl)}} , \quad (45)$$

or

$$\frac{T_{max}^{(growth)} - T_{max}^{(nucl)}}{T_m} \cong \left(\frac{2W_c}{3W_c + E_D^{(eff)}} \right) \Bigg|_{T=T_{max}^{(nucl)}} - \left(\frac{k_B T_m}{E_D^{(eff)}} \right) \Bigg|_{T=T_{max}^{(growth)}} . \quad (46)$$

For the special case of temperature-independent activation energies, the latter relation yields

$$\frac{T_{max}^{(growth)} - T_{max}^{(nucl)}}{T_m} \cong \frac{k_B T_m}{E_D} \left\{ 2 \left(\frac{W_c}{k_B T_m} \right) \left(\frac{1}{1 + \frac{3W_c}{E_D}} \right) - 1 \right\} \Bigg|_{T=T_{max}^{(nucl)}} . \quad (47)$$

Near $T_{max}^{(nucl)}$ the quantities W_c and E_D must be of similar order of magnitude. Indeed, $T_{max}^{(nucl)}$ specifies the temperature range in which the kinetic term $\exp(-E_D/k_BT)$ becomes dominant with decreasing temperature as compared to the thermodynamic term $\exp(-W_c/k_BT)$. For homogeneous nucleation, moreover, $(W_c/k_BT) \gg 1$ typically holds. Therefore, the maximum of the growth rate must be located in such cases at higher temperatures than the maximum of the homogeneous nucleation rate. This result is illustrated in Fig. 3, which shows the typical locations of the temperatures at maximum nucleation and growth rates for such cases. Although this experimental result is well known, to the best of our knowledge, this is the first time that a theoretical explanation such as the one given above has been developed.

The situation with respect to the location of the temperatures at maximum nucleation and growth rates may be quite different for heterogeneous nucleation (or similarly, systems that undergo homogeneous nucleation but whose specific interfacial energy is relatively low, cf. Eq. (8)) as illustrated in Fig. 4. In such cases, the maximum nucleation rates may even be located at higher temperatures than the maximum growth rates. Note that, in Figs. 3 and 4, the curves are given in reduced coordinates $(J(T)/J_{max}(T_{max}^{(nucl)})$. and $u(T)/u(T_{max}^{(growth)}))$. Thus, they do not reflect the dependence of the magnitudes of the nucleation and growth rates on temperature but only the possible different locations of the maxima along the temperature axis.

According to Eq. (1), the magnitudes of the steady-state nucleation rates are affected by the number of particles that may act as centers of nucleation (the number of particles, c, per unit volume for homogeneous nucleation and the number, c_{het}, of solid nucleation cores for

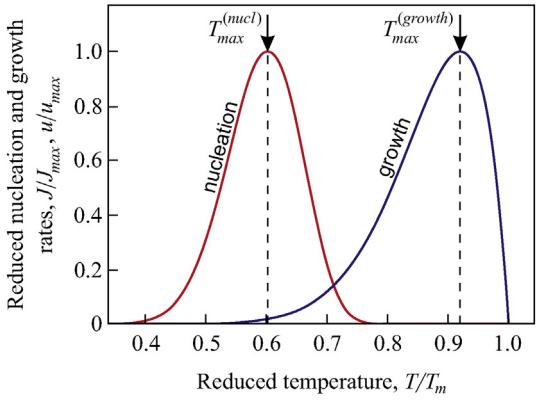

Fig. 3. Typical locations of the maxima of nucleation, $J = J(T)$, and growth, $u = u(T)$, rates in the case of homogeneous nucleation computed via Eqs. (4), (6), and (9). The values of the parameters employed in the computations are: $d_0 = 3.895 \cdot 10^{-10}$ J/K, $T_m = 1474$ K, $q = 1.24 \cdot 10^{-19}$ J, $\sigma = 0.15$ J/m^2, and $E_D = 1.6 \cdot 10^{-19}$ J.

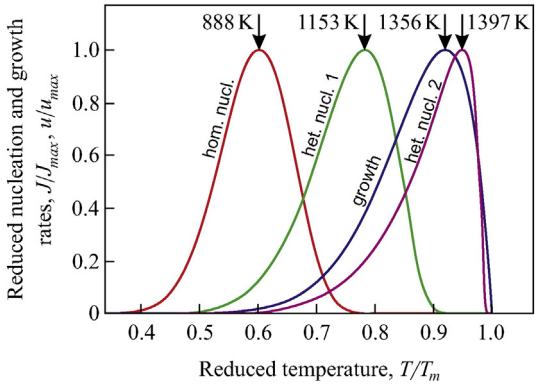

Fig. 4. Possible locations of the maxima of nucleation and growth rates for the case of heterogeneous nucleation which are computed, again, via Eqs. (4), (6), and (9). Here the possibility may be realized that the maximum of the nucleation rate is located at higher temperatures as compared to the growth rate. The following values are assumed for the nucleation activity of the nucleation cores: (1) $\Phi = 0.1$ and (2) $\Phi = 0.001$. Homogeneous nucleation may result in a similar picture if the specific surface energy has very low values (cf. Eq. (8)). The values of the other parameters employed in the computations are, again: $d_0 = 3.895 \cdot 10^{-10}$ J/K, $T_m = 1474$ K, $q = 1.24 \cdot 10^{-19}$ J, $\sigma = 0.15$ J/m^2, and $E_D = 1.6 \cdot 10^{-19}$ J. The blue growth curve describes the growth rate of clusters as far as they have already been formed by prior nucleation. Nucleation could occur on the cooling path from the liquid state or on the heating path to the desired temperature. If no nuclei are formed in these conditions, then, of course, there would be no growth.

heterogeneous nucleation). As a rule, $c_{het} \ll c$ holds. Consequently, heterogeneous nucleation may compete with homogeneous nucleation only in cases when the nucleation activity is considerably lower than one ($\Phi \ll 1$) (cf. also [3]). Therefore, in Fig. 4, this parameter was taken to be equal $\Phi = 0.1$ and $\Phi = 0.001$.

3.4. Maximum overall crystallization rate

According to the Johnson–Mehl–Avrami–Kolmogorov approach (cf. [2,3]) to the determination of the volume fraction, $\alpha_n(t)$, of the crystalline phase as a function of time, the maximum rate, $(d\alpha_n(t, T)/dt)$, of overall crystallization as a function of temperature (at any given value of crystal volume fraction, α_n, and time, t) is determined by the product $J(T)u^n(T)$:

$$\alpha_n(t,T) = 1 - \exp\left(-\frac{\omega_n}{(n+1)} J u^n t^{n+1}\right). \tag{48}$$

Here, n is the number of independent directions of growth and ω_n is a shape factor. Consequently, the maximum rate of overall crystallization as a function of temperature is defined by the relation

$$\frac{d}{dT}(Ju^n)\Big|_{T=T_{max}^{(overall)}} = 0, \tag{49}$$

resulting in

$$\left\{\frac{dJ}{dT}u + (Jn)\frac{du}{dT}\right\}\Big|_{T=T_{max}^{(overall)}} = 0. \tag{50}$$

Because u, J, and n are positive quantities, it follows from Eq. (50) that the maximum of the rate of overall crystallization is located at temperatures in between that of the maximum growth rate and that of the maximum nucleation rate (the derivatives (dJ/dT) and (du/dT) must have different signs). This result is intuitively evident and consistent with experimental observations.

With the same approximations used earlier (neglecting the temperature dependence of the pre-exponential terms) and employing Eqs. (4), (5) and (10), we obtain

$$\frac{d}{dT}\left(\frac{W_c + (n+1)E_D}{T}\right)\Big|_{T=T_{max}^{(overall)}} = n\left\{\frac{\exp\left(-\frac{\Delta\mu}{k_BT}\right)}{1-\exp\left(-\frac{\Delta\mu}{k_BT}\right)}\right\}\frac{d}{dT}\left(\frac{\Delta\mu}{T}\right)\Big|_{T=T_{max}^{(overall)}}. \tag{51}$$

Straightforward algebraic transformations yield

$$\frac{d}{dT}\left(\frac{W_c + (n+1)E_D}{T}\right) = -\frac{1}{T^2}\left\{W_c\frac{\left(1-3\frac{T}{T_m}\right)}{\left(1-\frac{T}{T_m}\right)} + (n+1)E_D^{(eff)}\right\}, \tag{52}$$

$$\frac{d}{dT}\left(\frac{\Delta\mu}{T}\right) = -\frac{q}{T^2}\ , \tag{53}$$

resulting in

$$\frac{T_{max}^{(overall)}}{T_m} = \frac{1-\Upsilon}{3-\Upsilon}\Big|_{T=T_{max}^{(overall)}}, \tag{54}$$

$$\Upsilon\left(T_{max}^{(overall)}\right) = (n+1)\frac{E_D^{(eff)}\left(T_{max}^{(overall)}\right)}{W_c\left(T_{max}^{(overall)}\right)} \times \times\left\{\frac{nq}{(n+1)E_D^{(eff)}\left(\exp\left(\frac{\Delta\mu}{k_BT}\right)-1\right)} - 1\right\}\Big|_{T=T_{max}^{(overall)}}. \tag{55}$$

3.5. Modification of the results when using the Stokes–Einstein–Eyring equation

In applications of the classical theory of nucleation and growth processes, the diffusion coefficient, D, governing nucleation and growth is usually not known and is therefore frequently estimated via the Stokes–Einstein–Eyring (SEE) relation [3]:

$$D \cong D_\eta = \gamma\frac{k_BT}{d_0\eta}. \tag{56}$$

This equation allows one to replace the diffusion coefficient, D, with the Newtonian viscosity, η. The parameter γ is a constant. Its value depends on the theoretical concepts and approximations employed in the derivation, and on the way of specification of the size parameter, d_0, of the basic molecular units of the melt utilized. Provided that Eq. (56) holds, D can be replaced by the viscosity, which is described by a relation similar to Eq. (5):

$$\eta = \eta_0\ \exp\left(\frac{E_\eta}{k_BT}\right), \tag{57}$$

with

$$E_D(T) = E_\eta(T). \tag{58}$$

All the relations obtained here for the location and magnitude of the maxima of the nucleation and growth rates remain the same; however, D must be replaced by $(1/\eta)$ via Eq. (56), $E_D(T)$ must be replaced by $E_\eta(T)$ and $E_D^{(eff)}(T)$ must be replaced by $E_\eta^{(eff)}(T)$ which is defined similarly to Eq. (15) by

$$E_\eta^{(eff)}(T) = \left(E_\eta(T) - T\frac{dE_\eta(T)}{dT}\right). \tag{59}$$

Provided the SEE-equation (and its consequence, Eq. (58)) hold, our analysis described in Sections 3.1 and 3.2 (high activation energies at T_m result in higher values of $T_{max}^{(nucl)}$ and in lower values of J_{max}; the growth rate decreases with increasing viscosity, i.e., increasing activation energy for viscous flow) offers an explanation of experimental results discussed by Tammann [26]. Tammann stated that "*the higher the melt viscosity at the melting temperature, the lower its crystallizability*" (cf. also Fig. 5a in [25] which provides additional support to Tammann's suggestion). However, as we have demonstrated here, crystallizability is affected not only by the activation energy at the melting temperature but also by the rate of change of the activation energy with temperature (cf. Eq. (16)).

4. Summary of results and discussion

The main results of the present analysis can be summarized as follows: (i) General relations for the location and magnitude of the maxima of the steady-state nucleation rate as a function of temperature have been derived (Eqs. (12) and (21), (17) and (23)). The ratio $T_{max}^{(nucl)}/T_m$ is determined exclusively by the work of critical cluster formation and the effective activation energy for diffusion. (ii) The magnitude of the maximum steady-state nucleation rate decreases with an increase of the ratio $T_{max}^{(nucl)}/T_m$ (cf. Eqs. (21) and (22) and Fig. 1). (iii) General relations are derived for the ratio $T_{max}^{(growth)}/T_m$ of the maximum growth rate and melting temperatures. $T_{max}^{(growth)}/T_m$ is defined by the interplay of the thermodynamic driving force for crystallization and the effective activation energy for diffusion at $T_{max}^{(growth)}$. The maximum growth rate decreases with increasing values of the ratio $T_{max}^{(growth)}/T_m$ (Eqs. (43) and (44)). The theoretical results allow for an accurate description of experimental data. (iv) The analytical expressions for $T_{max}^{(nucl)}/T_m$ and $T_{max}^{(growth)}/T_m$ are employed to estimate the sign and magnitudes of the differences of the temperatures at the maximum nucleation and growth rates. Consistent with experimental results, we observe that the maxima of the growth rates are located at higher temperatures than the maxima of the homogeneous nucleation rates (Eq. (47)). This conclusion holds provided the systems are characterized by typical values of the specific interfacial energy. Homogeneous nucleation in systems with a very small surface energy and heterogeneous nucleation may exhibit an opposite type of behavior. This conclusion is also in accordance with experimental observations. (v) The temperature at the maximum overall crystallization rate is shown to be located between the temperatures of the maximum nucleation and growth rates (Eqs. (50), (54) and (55)). This result is, again, in agreement with experimental observations. (vi) When the Stokes–Einstein–Eyring equation holds, in the equations determining the maximum rates of nucleation, growth, and overall crystallization (e.g., Eqs. (17), (34), and (47)), the effective activation energies for diffusion may be replaced by the effective activation energies for Newtonian viscosity.

In the present analysis, the classical theory of nucleation and growth is employed adapted to crystallization of one-component systems. However, all the basic relations remain valid for multi-component systems when crystallites are formed with a fixed stoichiometric composition that does not vary with cluster size (cf. [12,27,28]). Modifications are possible if some of the simplifying assumptions are replaced by more appropriate considerations. In particular, the state of the critical clusters in nucleation may differ from that of the evolving macroscopic phase. In such cases, the expression for the driving force of phase formation must be substantially modified. Other effects may also have to be taken into account [3,13,14] which are connected with peculiarities of crystallization at deep undercooling. However, it is believed that the general trends established here may be used as a guide even in such more complex situations.

In order to further develop the theory presented here, in particular, we will employ the general results derived by as the starting point for the analysis of the interplay of crystallization and glass transition and of the effects of fragility [29] and decoupling [30] on crystallization. Methods of specification of the decoupling temperature, which are based exclusively on the knowledge of directly measurable quantities (viscosity, crystal growth rate), will be developed in [30]. Specific features of crystal nucleation and growth at deep undercooling will be discussed in [31].

5. Conclusions

Relations have been developed to describe the main characteristics of crystallization processes. In particular, a set of equations for determining the temperatures and magnitudes of the maximum nucleation, growth, and overall crystallization rates of glass-forming liquids was derived and analyzed. These results can be applied to specific systems introducing appropriate models and relations for their thermodynamic and kinetic parameters. Moreover, the derived results also allow one to test different concepts advanced to describe the crystallizability of glass-forming melts in cooling, such as the correlation between glass-transition temperature and temperature at maximum nucleation rate, or between fragility and glass-forming ability. These topics will be addressed in a forthcoming paper.

Acknowledgments

The authors gratefully acknowledge the financial support from the German Academic Exchange Council (DAAD, Project No. A/14/02369) and of the Heisenberg-Landau program of the German Ministry of Science and Technology (BMBF). Generous and continuous funding by the Brazilian agencies CAPES, CNPq and São Paulo Research Foundation, FAPESP (CEPID Grant No. 13/07793-6) is greatly appreciated as well.

References

[1] W. Höland, G.H. Beall, Glass-Ceramic Technology, Second edition Wiley, New Jersey, 2012.
[2] K.F. Kelton, A.L. Greer, Nucleation in Condensed Matter: Applications in Materials and Biology, Pergamon, Amsterdam, 2010.
[3] I.S. Gutzow, J.W.P. Schmelzer, The Vitreous State: Thermodynamics, Structure, Rheology, and Crystallization, First edition Springer, Berlin, 1995 (Second enlarged edition, Springer, Heidelberg, 2013).
[4] C. Schick, et al., Influence of thermal prehistory on crystal nucleation and growth in polymers, in: J.W.P. Schmelzer (Ed.), Glass: Selected Properties and Crystallization, de Gruyter, Berlin 2014, pp. 1–93.
[5] G. Wilde, Early stages of crystal formation in glass-forming metallic alloys, in: J.W.P. Schmelzer (Ed.), Glass: Selected Properties and Crystallization, de Gruyter, Berlin 2014, pp. 95–136.
[6] V.M. Fokin, E.D. Zanotto, N.S. Yuritsyn, J.W.P. Schmelzer, J. Non-Cryst. Solids 352 (2006) 2681.
[7] P.W. Bridgeman, Rev. Mod. Phys. 18 (1) (1946).
[8] G. Tammann, Z. Phys. Chem. 25 (1898) 441.
[9] L.S.A. Gallo, T.M. Mosca, B.H. Teider, I.G. Polyakova, A.C.M. Rodrigues, E.D. Zanotto, V.M. Fokin, J. Non-Cryst. Solids 408 (2014) 102.
[10] E. Zhuravlev, J.W.P. Schmelzer, A.S. Abyzov, V.M. Fokin, R. Androsch, C. Schick, Cryst. Growth Des. 15 (2015) 786.
[11] V.G. Baidakov, Crystallization of undercooled liquids: results of molecular dynamics simulations, in: J.W.P. Schmelzer (Ed.), Glass: Selected Properties and Crystallization, de Gruyter, Berlin 2014, pp. 481–520.
[12] J.W.P. Schmelzer, J. Non-Cryst. Solids 354 (2008) 269 (**356**, 2901 (2010)).
[13] J.W.P. Schmelzer, V.M. Fokin, A.S. Abyzov, E.D. Zanotto, I. Gutzow, Int. J. Appl. Glas. Sci. 1 (2010) 16.
[14] G. Johari, J.W.P. Schmelzer, Crystal nucleation and growth in glass-forming systems: some new results and open problems, in: J.W.P. Schmelzer (Ed.), Glass: Selected Properties and Crystallization, de Gruyter 2014, pp. 521–585.
[15] G. Strobl, Rev. Mod. Phys. 81 (2009) 1287.
[16] T. Yamamoto, Polymer 50 (2009) 1975.
[17] V.M. Fokin, E.D. Zanotto, J.W.P. Schmelzer, O.V. Potapov, J. Non-Cryst. Solids 351 (2005) 1491.
[18] V.M. Fokin, E.D. Zanotto, J.W.P. Schmelzer, J. Non-Cryst. Solids 356 (2005) 2185.
[19] J.W.P. Schmelzer, E.D. Zanotto, I. Avramov, V.M. Fokin, J. Non-Cryst. Solids 352 (2006) 434.
[20] I. Markov, Crystal Growth for Beginners: Fundamentals of Nucleation, Crystal Growth and Epitaxy, World Scientific, Singapore, 2002.
[21] V.G. Baidakov, S.P. Protsenko, A.O. Tipeev, J. Chem. Phys. 139 (2013) 224703.
[22] Ya.I. Frenkel, The Kinetic Theory of Liquids, Oxford University Press, Oxford, 1946.
[23] V.N. Filipovich, Initial stages of crystallization of glasses and the formation of sitals, The Vitreous State, Academy of Sciences Publishers USSR, Moscow-Leningrad 1963, pp. 9–24.

[24] V.M. Fokin, A.M. Kalinina, V.N. Filipovich, J. Cryst. Growth 52 (1981) 115.
[25] J. Orava, A.L. Greer, J. Chem. Phys. 140 (2014) 214504.
[26] G. Tammann, Z. Elektrochem. 10 (1904) 532.
[27] V.V. Slezov, J.W.P. Schmelzer, Phys. Rev. E 65 (2002) 031506.
[28] V.V. Slezov, Kinetics of First-Order Phase Transitions, Wiley-VCH, Berlin-Weinheim, 2009.
[29] J.W.P. Schmelzer, A.S. Abyzov, V.M. Fokin, C. Schick, E.D. Zanotto, Crystallization in Glass-forming Liquids: Effects of Fragility and Glass Transition Temperature, J. Non-Cryst. Solids 428 (2015) 68.
[30] J.W.P. Schmelzer, A.S. Abyzov, V.M. Fokin, C. Schick, E.D. Zanotto, Crystallization in Glass-forming Liquids: Effects of Decoupling of Diffusion and Relaxation, 2015 (in press).
[31] V.M. Fokin, A.S. Abyzov, E.D. Zanotto, D. Cassar, A.M. Rodrigues, J.W.P. Schmelzer, Crystal Nucleation in Glass-forming Liquids: New Insights on Old Problems, 2015 (in preparation).